Fe₃O₄@Polydopamine Core-Shell Nanocomposite as a Sorbent for Efficient Removal of Rhodamine B from Aqueous Solutions: Kinetic and Equilibrium Studies

Baghban, Ali*⁺; Jabbari, Mohammad; Rahimpour, Elaheh

Department of Chemistry, Faculty of Science, Payame Noor University, P.O. Box 19395-3697 Tehran, I.R. IRAN

ABSTRACT: *In this work, a Fe₃O₄@polydopamine core-shell nanocomposite (Fe₃O₄/PDA) was synthesized through an in situ self-polymerization methods and was applied as a sorbent for Rhodamine B (RhB) removal. The synthetic procedure is simple and involves no organic solvents. The as-prepared Fe₃O₄/PDA nanocomposite was characterized by transmission electron microscope, Fourier transforms infrared spectra, and X-ray photoelectron spectroscopy. Due to the catechol and amine groups, the polydopamine (PDA) polymer provided multiple interactions in combination with RhB. The removal ratios of the RhB by Fe₃O₄/PDA were all above 98% at the optimum experimental conditions, suggesting that the Fe₃O₄/PDA nanocomposite was an excellent sorbent for acid dyes removal from aqueous solution. The kinetic studies revealed that sorption follows a pseudo-second order kinetic model which indicates chemisorption between sorbent and adsorbate molecules. The Langmuir adsorption models were applied to describe the equilibrium isotherms, and the isotherm constants were also determined. The maximum adsorption capacity derived from the Langmuir model was 195.3 mg/g.*

KEYWORDS: *Magnetic polydopamine nanocomposite; Core-shell; Absorbent; Rhodamine B.*

INTRODUCTION

Organic dyes which could generate a lot of toxic substances are familiar pollutants in wastewaters. The rapidly growing in the use of synthetic dyes in many fields of advanced technology, e.g., in various kinds of the textile, paper, leather tanning, food processing, plastics, cosmetics, rubber, printing, and dye manufacturing industries has led to a significant increase in environmental pollution [1]. Many of these dyes are toxic and their exposure poses serious environmental, aesthetical and health problems. Therefore, they should be removed from wastewater before being discharged into water resources in order to protect the living organisms.

Rhodamine B ((C₂₈H₃₁N₂O₃Cl; mol. wt. 479; IUPAC Name N-[9-(ortho-carboxyphenyl)-6-(diethylamino)-3H-xanthen-3-ylidene] diethyl ammonium chloride), RhB), a synthetically prepared carcinogenic basic red dye of the xanthene class is widely used as a colorant in the textile, foodstuffs, a well-known water tracer fluorescent, and

also as a biological stain in the laboratory [2, 3]. It causes irritation of the skin, eyes and respiratory tract and is implicated in causing carcinogenicity, reproductive and developmental toxicity, neurotoxicity and chronic toxicity toward humans and animals [4]. Therefore, keeping the hazardous nature and harmful effects in view, it was considered worthwhile to make systematic efforts to remove Rhodamine B from wastewaters.

To date, several technologies have been developed for dye removal including coagulation and flocculation [5], membrane [6], ozonation [7], electrochemical [8], and adsorption [9, 10]. Among these available methods, adsorption is found to be the most effective treatment for the removal of metal ions, dye and any other pollutant like as radioactive wastes from industrial wastewaters, due to its high efficiency, simplicity, easy to perform, and insensitive to toxic substances [11, 12]. Commonly used sorbents can suffer from low sorption capacities and separation inconveniences. Therefore, the exploration of new promising adsorbents is still desirable.

Dopamine (2-(3, 4-dihydroxyphenyl)ethylamine, DA) is a small molecule mimic of the adhesive proteins that contains catechol and amine functional groups [13]. Messersmith's group reported that DA can be self-polymerized in aerated basic media [14]. During polymerization, PDA will spontaneously form a conformal and continuous coating layer atop nearly any material present in the reaction media. This approach, originally inspired by the adhesive properties displayed by mussels, was introduced in the past decade and shown to generate a range of polydopamine (PDA)-coated planar substrates including noble metals, metal oxides, semiconductors, ceramics, and synthetic polymers via the strong binding affinity of catechol functional groups [13, 15]. The advantage of PDA modification lies in its easy, convenience and substantial-independence [16]. Due to their unique properties such as extraordinary biocompatibility, multifunctional groups (amino and catechol groups), excellent dispersibility in water and providing π–π stacking interaction to targets, PDA coated material are currently considered as effective, efficient, economic and eco-friendly sorbents for removal of both organic and inorganic pollutants [17]. Using of Fe_3O_4 nanoparticles, as a substrate for PDA, enables us to acquire a sorbent with magnetic recyclability property. These magnetic nanocomposites can be conveniently

collected from the solution by applying an external magnetic. Magnetic separation has been one of the promising techniques for environmental water purification and separation because of its producing no contaminants such as flocculants and having the capability of treating a large amount of wastewater within a short time [18]. Moreover, this approach is particularly desirable in the industry because it can overcome many of the issues present in centrifugation, filtration or gravitation separation [19].

In this study, a high efficient magnetic adsorbent material prepared by modifying Fe_3O_4 magnetic nanoparticles with PDA was developed for removal of RhB from wastewaters. The synthesis of Fe_3O_4@polydopamine (Fe_3O_4/PDA) nanocomposite was discussed, together with their physical and chemical properties. The adsorption characteristics and the effect of some experimental factors such as sorption kinetic and capacity, effects of pH, contact time, as well as the adsorbent dosage was investigated in detail in batch experiments. It can be seen, Fe_3O_4/PDA nanocomposite shows nearly complete (over 98 %) RhB removal, as a practical approach for dye separation from wastewaters.

EXPERIMENTAL SECTION
Chemicals and materials

All chemicals used in the experiment were of analytical grade and used without further purification. The high-purity deionized water was used throughout the experiment. Dopamine hydrochloride was purchased from Sigma–Aldrich Chemie (Madrid, Spain). Ferric chloride hexahydrate ($FeCl_3 \cdot 6H_2O$), and ferrous chloride ($FeCl_2 \cdot 4H_2O$), ammonia solution (NH_3), sodium hydroxide (NaOH) and hydrochloric acid (HCl) used for pH adjustment and other chemicals used in the experiment were also purchased from Merck (Darmstadt, Germany). A stock solution of RhB (200 mg/L) was prepared by dissolving solid RhB in water, and kept at 4 °C in a refrigerator.

Instrumentation

In order to identify the crystal structure of as-prepared nanoparticles, powder X-Ray 124 Diffraction (XRD) measurement were performed by employing a Bruker D8 Advance (Bruker AXS, Karlsruhe, Germany) instrument with Cu-K$_\alpha$ radiation source (1.54 Å) between 10 and 70°

18

generated at 40 kV and 35 mA at room temperature. In addition, FT-IR spectra (4000-400 cm^{-1}) was recorded on a Vector 22 (Bruker, Ettlingen, Germany) Fourier transform infrared spectrometer using the KBr pellet with a ratio sample/KBr of 1:100 by mass. The morphology of Fe₃O₄/PDA was characterized by transmission electron microscope model 906 E (Zeiss, Göttingen, Germany). The concentrations of dye solutions were measured using a UV-2501 spectrophotometer.

Preparation of Fe₃O₄/PDA magnetic nanocomposite
Synthesis of Fe₃O₄ nanoparticles

The magnetic Fe₃O₄ nanoparticles were synthesized by the following chemical co-precipitation method. 11.68 g of FeCl₃·6H₂O and 4.30 g of FeCl₂·6H₂O were dissolved in 200 mL of high purity water under nitrogen gas with vigorous stirring at 353 K. Then, 40 mL of 30% (v/v) ammonia solution was added with further increased nitrogen passing rate and stirring speeds, the orange-red clear solution became a black suspension immediately. The pH of the final mixture adjusted in the range of 11–12. To promote the complete growth of the nanoparticle crystals, the reaction was carried out at 353 K for 1 h under constant mechanical stirring and the obtained suspension was cooled down to room temperature. After cooling to room temperature, the obtained precipitate was collected with the help of a magnet and washed thoroughly with deionized water for several times until the pH became 7.

Synthesis of Fe₃O₄/PDA nanocomposite

Fe₃O₄/PDA nanocomposite was prepared as follows: Briefly, 300 mg of as-prepared Fe₃O₄ nanoparticles and 100 mg dopamine hydrochloride were dissolved in 50 mL tris-buffer (pH 8.5) solution and allowed to proceed for 24 h at room temperature under stirring. The resulted nanocomposite was sequentially washed with ethanol and water several times and dried under vacuum at 70 °C overnight [20].

Adsorption experiments

Batch-mode adsorption studies were carried out by adding 0.4 g/L Fe₃O₄/PDA nanocomposite to 20 mL of dye solutions in the concentration range from 10 to 90 mg/L in a beaker. The mixture was sonicated for 40 minutes in an ultrasonic bath at a constant temperature to form a homogeneous suspension. After that, Fe₃O₄/PDA nanocomposite was magnetically separated by placing an Nd-Fe-B strong magnet at the bottom of the beaker. Finally, the equilibrium concentration of the dyes in the supernatant solution was determined by UV-Vis spectrophotometer. The removed quantity (q_{eq} in mg/L) of the dye by the Fe₃O₄/PDA sorbent was calculated by the following equation:

$$q_{eq} = \frac{C_0 - C_{eq}}{m} V \qquad (1)$$

Where C_0 (mg/L) represents the initial dye concentration, C_{eq} (mg/L) is the equilibrium concentration of the dye remaining in the solution, V (L) is the volume of the aqueous solution, and m (g) is the weight of the sorbent.

Adsorption kinetic experiments were conducted to find out the equilibrium time and the kinetic models of RhB sorption by Fe₃O₄/PDA: aliquots of 20 mL of 20 mg/L dye solutions containing 0.1, 0.2, 0.4, 0.6, and 0.8 g/L of Fe₃O₄/PDA, were prepared in glass beakers. The beakers were placed in an ultrasonic bath. At certain time intervals of sonicating, the Fe₃O₄/PDA was separated and removed from the solution by magnetic separation. The remaining concentration of the dye in the supernatant solution was then determined by UV–Vis spectrometry.

The effect of the solution pH on the dye removal was studied by adjusting the pH of the solution from 3 to 10 with 0.1 mol/L HCl or 0.1 mol/L NaOH. To investigate the effect of the nano sorbent amount on the adsorption, different amounts of the Fe₃O₄/PDA (2~16 mg) were added to 20 mL of RhB solution (20 mg/L) and experiments were conducted by a mentioned method in above. Dye adsorption isotherms were studied at the sample solution with an initial pH of 7.0 ±0.2. The concentration of the Fe₃O₄/PDA was 0.4 g/L and the dye concentration was varied from 10 to 100 mg/L. The effect of temperature on the adsorption of RhB by Fe₃O₄/PDA was investigated by controlling the temperature at 283 to 323 K.

RESULTS AND DISCUSSION
Characterization of Fe₃O₄/PDA nanocomposite

The crystal structures of the obtained Fe₃O₄ and Fe₃O₄/PDA nanocomposite were characterized by X-Ray Diffraction (XRD). Fig. 1A shows the XRD patterns of

19

Fe_3O_4 and Fe_3O_4/PDA nanocomposite. For Fe_3O_4, a high-intensity sharp peak at $2\theta= 35.5°$ related to the (311) plane in the electron diffraction pattern. Five additional weak peaks at 30.1°, 43.1°, 54.4°, 57.0° and 62.6° corresponded to the (220), (440), (422), (511) and (440) planes, respectively. The results were matched well with the database of a face-centered cubic lattice of Fe_3O_4 (JCPDS card No. 19-629) [21]. Notably, the XRD pattern of the Fe_3O_4/PDA nanocomposite has similar diffraction peaks as those of bare Fe_3O_4, indicating that the polymer shell is amorphous in nature and the main magnetite phase of magnetic cores was not destroyed during the fabrication procedure and PDA was not changed the crystalline phase of Fe_3O_4 nanoparticles.

FT-IR was also carried out to verify the surface composition of the synthesized nanocomposites. FT-IR spectra of Fe_3O_4 and Fe_3O_4/PDA were shown in Fig. 1B. In the spectrum of bare Fe_3O_4, the strong peak at 575 cm^{-1} is related to the vibration of the Fe–O function group and the peaks at 1628 and 3441 cm^{-1} are corresponding to the surface-adsorbed water and hydroxyl groups. In the spectrum of PDA modified Fe_3O_4 nanoparticles, new peaks at $\sim$1250 cm^{-1}, $\sim$1500 $cm^{-1,}$ and $\sim$1600 cm^{-1} derive from the aromatic rings in the PDA polymer. The peak at $\sim$3400 cm^{-1} of Fe_3O_4/PDA nanocomposite is broader than that of Fe_3O_4 nanoparticles, which results from the overlapping of hydroxyls, water adsorbed in PDA polymer and amines of PDA [17, 22]. The adsorption peaks at 2923 cm^{-1}, 2920 cm^{-1} are ascribed to the bending vibration or stretching vibration of CH_2 and CH_3 species. A weak absorbance at $\sim$1710 cm^{-1} can be indicative of esters formed by reaction of the hydroxyl groups of Fe_3O_4 with catechol hydroxyl groups of PDA [22]. These results suggest that PDA polymer is successfully immobilized on the surface of Fe_3O_4 nanoparticles.

Additionally, the morphologies of as-synthesized nanocomposites were characterized by TEM (Fig. 1C). As can be seen, the uniform Fe_3O_4/PDA nanocomposite (15-20 nm) with a core-shell structure was successfully synthesized.

Adsorption studies

In order to explore adsorption characteristics, the Fe_3O_4/PDA was tested as the adsorbent for the removal of the organic dye RhB from aqueous solutions.

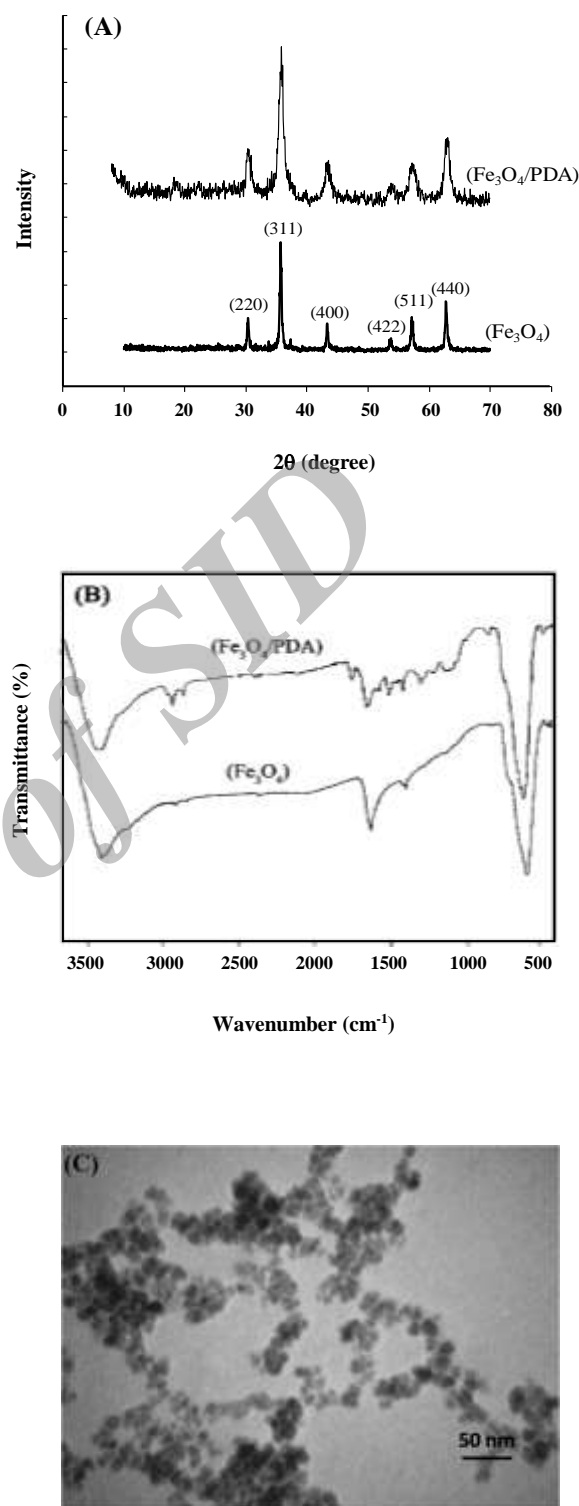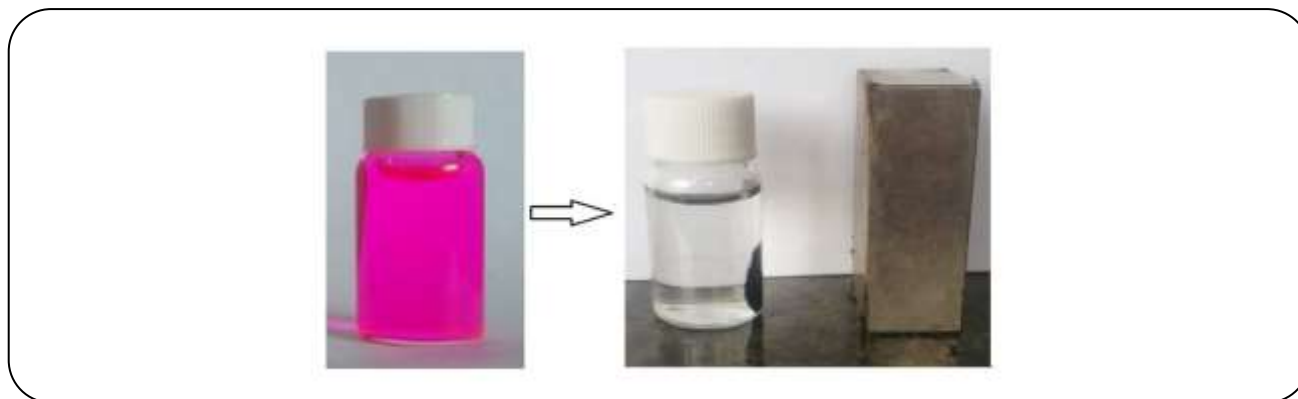Fig. 1: (A) XRD pattern (B) IR spectra of synthesized Fe₃O₄, Fe₃O₄/PDA, and (C) Typical TEM image of Fe₃O₄/PDA nanoparticles.

Fig. 2: Photograph of the RhB solution (20 mg L⁻¹, left) and the same solution after 40 min sonicated in the present of Fe₃O₄/PDA nanocomposite. The magnetic adsorbent was separated by the magnet (right).

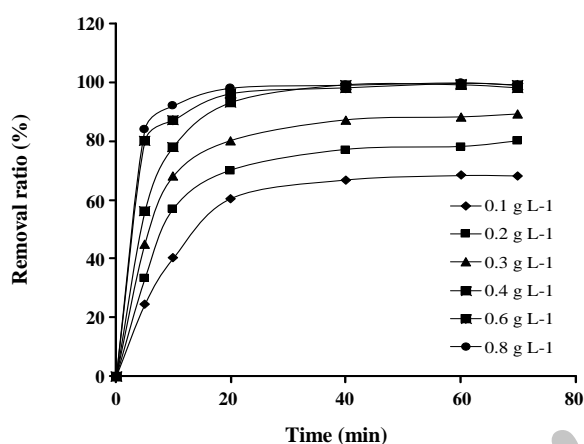*Fig. 3: Effect of Fe₃O₄/PDA dosage on the removal ratio of the RhB in water.*

It was observed that after the mixture of the Fe₃O₄/PDA and dye aqueous solution was sonicated for some period of time, the nanocomposite can be easily separated from the aqueous solution by placing a magnet outside of the glass bottle and the supernatant became nearly colorless. A schematic illustration of the adsorption procedure of the nanocomposite is shown in Fig. 2. Effects of parameters such as pH, adsorbent dose, contact time and temperature were studied.

Influence of Fe₃O₄/PDA dosage and time

In real condition, a good adsorbent should have the ability to remove the relatively higher amount of dye at its lower amount or on the other hands the adsorption process has been economical [23]. Therefore, the effect of adsorbent dose on the percentage adsorption of RhB onto Fe₃O₄/PDA nanocomposite was studied at a different dose ranging from 0.1 g/L to 0.8 g/L in neutral medium and is shown in Fig. 3. It can be seen that the percentages of the adsorbed dye increased as the Fe₃O₄/PDA dosage was increased over the range from 0.1 to 0.4 g/L and then it remains constant. The corresponding removal ratio of the RhB was increased from 64.1% to 99.2%. Thus, 0.4 g/L Fe₃O₄/PDA seems to be the optimum amount for the removal of RhB, and this dose was used in all subsequent experiments.

The effect of contact time on the adsorptions of RhB was also studied. At 0.4 g/L of the Fe₃O₄/PDA, about 56.6% of RhB was adsorbed within 5 min and 98.8% of RhB was adsorbed within 40 min. The results indicated that the RhB adsorption process occurred during the first few minutes and the adsorption equilibrium time for RhB was about 40 min.

Influence of pH

Solution pH is an important factor in the adsorption process, which not only influences the surface charge of adsorbent but also physicochemical properties of adsorbate [24]. The influence of aqueous solution pH on the adsorption capacity of RhB by the Fe₃O₄/PDA was studied over the pH range from 3 to 10. The results were shown in Fig. 4. The removal efficiencies of RhB were low at low pH, with increasing the solution pH to 7, the removal efficiencies of RhB enhanced dramatically to over 98.5%. As the point of zero charges of nanocomposite being located at pH 5.5 [25], at pH below the 7, the sorbent surface was protonated to get positive charges and in this pH range RhB existed as cationic, the electrostatic repulsion was unfavorable for these cations contacting with the positively charged surface for further interaction.
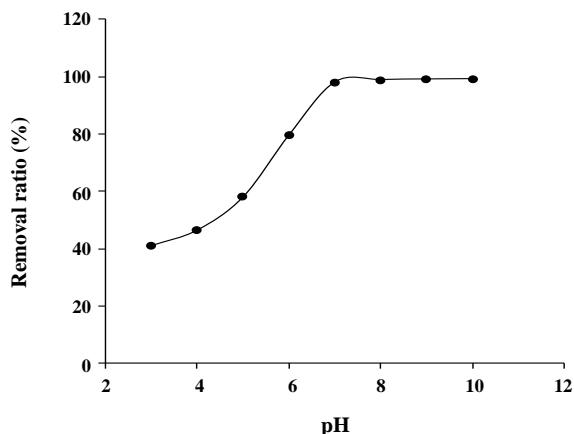
21

Fig. 4: Effect of initial solution pH on removal ratio of RhB.

Fig. 5: Van't Hoff plots of the RhB adsorption on the Fe₃O₄/PDA nanocomposite.

With solution pH increasing, the Fe$_3$O$_4$/PDA surface was deprotonated, and negative charge enhanced sharply. The electrostatic attraction facilitated contact cation pollutants and consequently result in their increased adsorption on the Fe$_3$O$_4$/PDA. When the pH values were increased from 7 to 10, the amount of RhB adsorbed was not significantly altered.

Influence of temperature on adsorption

The adsorption experiments at different temperatures were also performed to evaluate the influence of temperature (283–323 K). The thermodynamic property of the adsorbent-dye (Fe$_3$O$_4$/PDA – RhB) system was calculated using the Van't Hoff equation (Eq. (2)) [26].

$$\ln K_d = \frac{-\Delta H}{RT} + \frac{-\Delta S}{R} \qquad (2)$$

Where ΔS and ΔH are the values of the entropy change and the enthalpy change during the process, R (8.314 J/ mol.K) is the universal gas constant, T (K) is the absolute temperature and K_d is the distribution coefficient, which is expressed by (Eq. (3)) [27,28]:

$$K_d = \frac{q_e}{C_e} \qquad (3)$$

Fig. 5 shows the effect of temperature on the adsorption of RhB on Fe$_3$O$_4$/PDA. As can be seen, the amount of adsorbed dye decreased with the increase of temperature, as expected for an exothermic adsorption process. Plotting $\ln K_d$ against $1/T$ gives a straight line
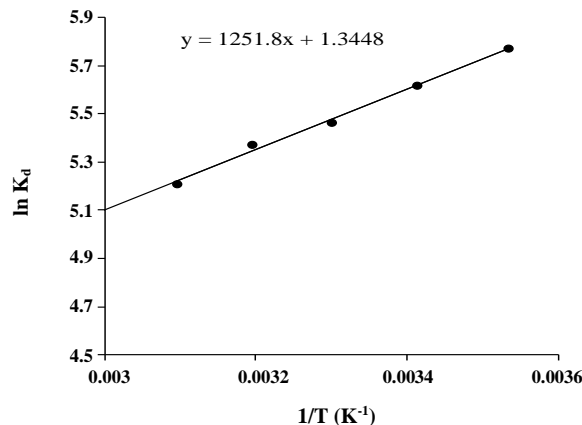
with slope and intercept equal to $-\Delta H/R$ and $\Delta S/R$, respectively. The negative value of H (Table 1) shows the exothermic nature of adsorption process. The adsorption was favored at a lower temperature and RhB molecules were orderly adsorbed on the surface of Fe$_3$O$_4$/PDA. Gibbs free energy of adsorption (ΔG) was calculated from the following relation:

$$\ln K_d = -\frac{\Delta G}{RT} \qquad (4)$$

$$\Delta G = \Delta H - T\Delta S \qquad (5)$$

The negative value of ΔG (Table 1) indicates that the adsorption reaction was spontaneous at 303, 313 and 323 K.

Kinetics analysis

Adsorption kinetics which provides the information about adsorption path and adsorption mechanism could evaluate adsorption performance of the absorbent [24]. In the present study, pseudo-first-order [29] and pseudo-second-order [30] kinetic models were used to fit the experimental data. The pseudo-first-order kinetic model is expressed by the following equation (Eq. (6)):

$$\ln(q_e - q_t) = \ln q_e - k_1 t \qquad (6)$$

Where q_t and q_e represent the amount of the dye adsorbed (mg/g) at any time t (min) and at equilibrium, respectively, and k_1 is the rate constant of adsorption (min^{-1}). Values of k_1 and q_e can be calculated from the slope and intercept of the plots of $\ln(q_e - q_t)$ versus t (Fig. 6A). The values of experimental q_e do not agree with

22

Table 1: Thermodynamic parameters of RB removal at different temperatures.

T/k	ΔG (kJ/mol)	ΔH (kJ/mol)	ΔS (J mol/K)
283	-2.123	-10.4	11.18
293	-2.235		
303	-2.347		
313	-2.459		
323	-2.571		
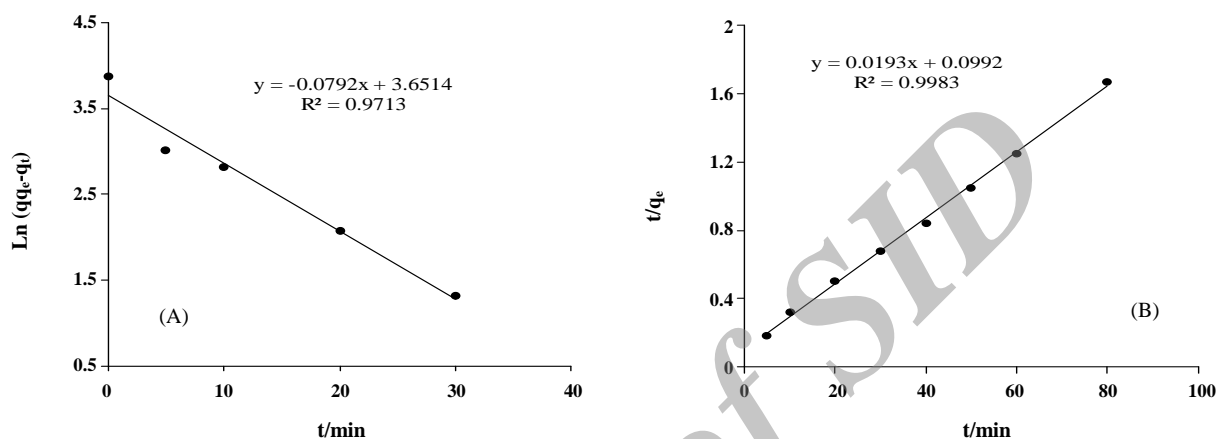
Fig. 6: Kinetic modeling of the adsorption process of RhB on Fe₃O₄/PDA; (A) Pseudo first order, (B) Pseudo-second order.

the calculated ones and the values of the correlation coefficient (R^2) are relatively low for most of the adsorption data (Table 2). This shows that the adsorption process may not be fitted with the first-order rate equation, correctly. Another kinetic model is pseudo-second-order model which can be expressed as (Eq. (7)):

$$\frac{t}{q_t} = \frac{1}{k_2 q_e^2} + \frac{1}{q_e} t \qquad (7)$$

Where K_2 is the rate constant for the pseudo-second-order adsorption process (g/mg min). The second order rate constant k and q_e could be determined from the intercept and slope of the plot obtained by plotting t/q_t versus t (Fig. 6B). As a result, a good linear relationship between t/q_t and t was obtained with the correlation coefficient (R^2) of 0.9983, which indicated that the adsorption kinetic follows the pseudo-second-order model. The calculated values of q_e and k were 51.8 mg g^{-1} and 0.0038 g/mg.min, respectively. The experimental q_e value is 48 mg/g, which agreed well with the q_e value calculated from the pseudo-second-order model.

According to the assumption of the pseudo-second-order model [31-33], it can be concluded from the experimental result that the adsorption of RhB on the Fe₃O₄/PDA is due to a chemical adsorption.

The Intra-particle diffusion model is described using the equation [34]:

$$q_t = K_p t^{0.5} + C \qquad (8)$$

Where K_p is intra-particle diffusion constant (mg/g min$^{0.5}$). This can be obtained from a plot of q_t versus $t^{0.5}$. The intercept that gives constant 'C' indicates whether the controlling step is intra-particle diffusion or not. If $C \neq 0$, the adsorption mechanism is quite complex. If $C = 0$, adsorption kinetics are only controlled by intra-particle diffusion [34, 35]. In this study, C is always a non-zero value revealing that the adsorption process is not controlled by intra-particle diffusion.

Adsorption isotherms

Equilibrium adsorption studies were performed to examine the adsorption capacities and mechanisms of

23

Table 2: Parameters of the kinetic models fitting to the experimental data.

Model	$q_{e,exp}$ (mg/g)	$q_{e,cal}$ (mg/g)	K	R^2
Pseudo-first-order	48	38.5	0.0792	0.9713
Pseudo-second-order	48	51.8	0.0037	0.9983

Table 3: Parameters based on the Langmuir and Freundlich isotherm equations and regression coefficients (r)
for the adsorption of RhB on Fe₃O₄/PDA at 298 K.

Langmuir	a_L (L/mg)	K_L (L/mg)	R^2	q_{max} (mg/g)	R_L
	0.9142	90.86	0.9917	195.3	0.05185
Freundlich	K_F (L/mg)	$1/n$	r		
	72.68	0.1576	0.977		

Fe₃O₄/PDA for RhB. To quantitatively describe the adsorption capacities, the two commonly used adsorption isotherms, Langmuir and Freundlich were applied. Equilibrium isotherm studies were carried out with different initial concentrations of RhB (from 10 to 100.0 mg/L) at 298 K. A relationship between the adsorption capacity of the Fe₃O₄/PDA nanocomposite and dye concentration can be expressed using the Langmuir adsorption equations as Eq. (9):

$$\frac{C_e}{q_e} = \frac{C_e}{q_{max}} + \frac{1}{q_{max} a_L} \tag{9}$$

Where C_e is the equilibrium concentration of the dye in the solution (mg/L), q_e is the amount of the dye adsorbed per unit mass of adsorbent (mg/g), q_{max} is the maximum adsorption at monolayer coverage (mg/g), which depends on the number of adsorption sites, a_L is the Langmuir adsorption equilibrium constant (L/mg) reflecting the energy of the adsorption. The values of q_{max} and a_L were calculated from the slope and intercept of the plot of C_e/q_e vs. C_e.

The parameters of the Langmuir equation were calculated and given in Table 3. The result indicated that the maximum adsorption capacity of Fe₃O₄/PDA, q_{max}, is 195.3 mg/g.

And the Freundlich model equation expressed as Eq. (10):

$$\ln q_e = \frac{1}{n} \ln C_e + \ln K_F \tag{10}$$

Where K_F and $1/n$ are the Freundlich characteristic constants indicating the adsorption capacity and the adsorption intensity, respectively. The values of K_F and

$1/n$ can be obtained from the intercept and slope of the linear plot of $\ln q_e$ versus $\ln C_e$. The results were listed in Table 3.

The Langmuir adsorption isotherm [36] is often used to equilibrium adsorption assuming monolayer adsorption onto a surface with a finite number of identical sites which is no interaction between the adsorbed molecules. While the Freundlich isotherm model assumes heterogeneity of the adsorption surface, the results indicated that the linear correlation coefficients for both Freundlich and Langmuir models were larger than 0.977 and the correlation coefficients for the Langmuir model were higher, indicating that the Langmuir model might fit the adsorption data better than the Freundlich one. This indicated that the RhB could be adsorbed on the Fe₃O₄/PDA nanocomposite as a monolayer adsorption, and the Fe₃O₄/PDA nanocomposite exhibited a high adsorption capacity for the RhB dye.

Furthermore, the essential feature of the Langmuir isotherm can be expressed in terms of a dimensionless constant separation factor (R_L) given by the following equation (Eq. (11)):

$$R_L = \frac{1}{1 + a_L C_0} \tag{11}$$

The value of R_L indicates the shape of the Langmuir isotherm and the nature of the adsorption process. R_L values within the range $0 < R_L < 1$ indicate a favorable adsorption [37]. In this study, R_L value for the RhB adsorption on the Fe₃O₄/PDA at initial RhB concentration of 20.0 mg/L was 0.05185, indicating a favorable adsorption of RhB onto the Fe₃O₄/PDA. In addition,

Table 4: Maximum adsorption capacities for the adsorption of RhB onto various adsorbents.

Adsorbents	Adsorption capacity (mg/g)	References
Fe_3O_4/HA	161.8	38
Treated parthenium biomass	59.2	39
Modified parthenium biomass	18.5	40
Kaolinite	46.08	41
Duolite C-20 resin	28.57	42
Fe-bentonite	98.62	43
Fe_3O_4/MIL-100(Fe)	28.36	44
Graphene nanosheets	111.11	45
Casuarina equisetifolia needle	82.34	46
Zinc oxide loaded activated carbon	128.2	47
Animal bone meal	62.11	48
Fe_3O_4/PDA	195.3	This work

the low R_L values (<0.1) implied that the interaction of RhB with Fe_3O_4/PDA might be relatively strong.

Comparison of the adsorption efficiency of the Fe₃O₄/PDA with other adsorbents

Table 4 lists a comparison of the maximum adsorption capacity of the nano sorbent in this study with various adsorbents previously used for the removal of RhB [38-44]. It can be seen, the Fe_3O_4/PDA possess a higher adsorption capacity than the other adsorbents reported in the literature, indicating that it is an efficient adsorbent for the dye and can be potentially used as a magnetic adsorbent to remove dye contaminants from water.

CONCLUSIONS

In this work, Fe_3O_4@polydopamine core-shell nanocomposite (Fe_3O_4/PDA) was prepared through an in situ self-polymerization method, and its properties for removal of RhB from aqueous solution was investigated. The Fe_3O_4/PDA could be simply re-collected from water with magnetic separations within a few minutes. The adsorption process followed the Langmuir adsorption model and the maximum adsorption capacity of 195.3 mg/g was observed. The adsorption process was better described by the pseudo-second-order kinetic model than other kinetic models with high correlation coefficients. The effect of temperature revealed that the adsorption of the dye, RhB, is exothermic. The Fe_3O_4/PDA was able to remove 98.5% of RhB in water at pH 7, and this adsorbent was stable in solution with a high pH. Furthermore, in compared with another sorbent for RhB removal, Fe_3O_4/PDA nanocomposite was very effective and efficient for the adsorption of RhB dye from contaminated water due to its high adsorption capacity, very rapid adsorption, as well as simple and convenient magnetic separation.

REFERENCES

[1] Alaei M., Mahjoub A.R., Rashidi A., Effect of WO₃ Nanoparticles on Congo Red and Rhodamine B Photo Degradation, *Iranian Journal of Chemistry and Chemical Engineering (IJCCE),* **31**(4): 23-29 (2012).

[2] Das S.K., Ghosh P., Ghosh I., Guha A.K., Adsorption of Rhodamine B on Rhizopus Oryzae: Role of Functional Groups and Cell Wall Components, *Colloids and Surfaces B: Biointerfaces*, **65**: 30-34 (2008).

[3] Mohammadi M., Hassani A.J., Mohamed A.R., Najafpour G.D., Removal of Rhodamine B from Aqueous Solution Using Palm Shell-Based Activated Carbon: Adsorption and Kinetic Studies, *Journal of Chemical & Engineering Data*, **55**: 5777-5785 (2010).

25

[4] Nagaraja R., Kottam N., Girija C.R., Nagabhushana B.M., Photocatalytic Degradation of Rhodamine B Dye Under UV/Solar Light Using ZnO Nanopowder Synthesized by Solution Combustion Route, *Powder Technology*, **215–216**: 91-97 (2012).

[5] Guibal E., Roussy J., Coagulation and Flocculation of Dye-Containing Solutions Using a Biopolymer (Chitosan), *Reactive and Functional Polymers*, **67**: 33-42 (2007).

[6] Xu H., Liu D.d L., He L., Adsorption of Copper(II) from an Wastewater Effluent of Electroplating Industry by Poly(ethyleneimine)-Functionalized Silica, *Iranian Journal of Chemistry and Chemical Engineering (IJCCE),* **34**(2): 73-81(2015).

[7] Ahmadi S.H., Davar P., Manbohi A., Adsorptive Removal of Reactive Orange 122 from Aqueous Solutions by Ionic Liquid Coated Fe_3O_4 Magnetic Nanoparticles as an Efficient Adsorbent, *Iranian Journal of Chemistry and Chemical Engineering (IJCCE),* **35**(1): 63-73 (2016).

[8] Gupta V.K., Jain R., Varshney S., Electrochemical Removal of the Hazardous Dye Reactofix Red 3 BFN from Industrial Effluents, *Journal of Colloid and Interface Science*, **312**: 292-296 (2007).

[9] Ishaq M., Saee, K., Ahmad I., Sultan S., Coal Ash as a Low Cost Adsorbent for the Removal of Xylenol Orange from Aqueous Solution, *Iranian Journal of Chemistry and Chemical Engineering (IJCCE),* **33**(1): 53-58 (2014).

[10] Foo K.Y., Hameed B.H., Preparation of Activated Carbon from Date Stones by Microwave Induced Chemical Activation: Application for Methylene Blue Adsorption, *Chemical Engineering Journal*, **170**: 338-341 (2011).

[11] Guo J., Wang R., Tjiu W.W., Pan J., Liu T., Synthesis of Fe Nanoparticles@Graphene Composites for Environmental Applications, *Journal of Hazardous Materials*, **225–226**: 63-73 (2012).

[12] Miao Y.E., Wang R., Chen D., Liu Z., Liu T., Electrospun Self-Standing Membrane of Hierarchical $SiO_2@\gamma$-AlOOH (Boehmite) Core/Sheath Fibers for Water Remediation, *ACS Applied Materials & Interfaces*, **4**: 5353-5359 (2012).

[13] Zhao Y., Yeh Y., Liu R., You J., Qu F., Facile Deposition of Gold Nanoparticles on Core–Shell Fe_3O_4@Polydopamine as Recyclable Nanocatalyst, *Solid State Sciences*, **45**: 9-14 (2015).

[14] Lee H., Rho J., Messersmith P.B., Facile Conjugation of Biomolecules onto Surfaces via Mussel Adhesive Protein Inspired Coatings, *Advanced Materials*, **21**: 431-434 (2009).

[15] Lee H., Dellatore S.M., Miller W.M., Messersmith P.B., Mussel-Inspired Surface Chemistry for Multifunctional Coatings, *Science*, **318**: 426-430 (2007).

[16] Ye Q., Zhou F., Liu W., Bioinspired Catecholic Chemistry for Surface Modification, *Chemical Society Reviews*, **40**: 4244-4258 (2011).

[17] Wang Y., Wang S., Niu H., Ma Y., Zeng T., Cai Y., Meng Z., Preparation of Polydopamine Coated Fe_3O_4 Nanoparticles and Their Application for Enrichment of Polycyclic Aromatic Hydrocarbons from Environmental Water Samples, *Journal of Chromatography A*, **1283**: 20-26 (2013).

[18] Ambashta R.D., Sillanpää M., Water Purification Using Magnetic Assistance: A Review, *Journal of Hazardous Materials*, **180**: 38-49 (2010).

[19] Wu Q., Feng C., Wang C., Wang Z., A Facile One-Pot Solvothermal Method to Produce Superparamagnetic Graphene–Fe_3O_4 Nanocomposite and Its Application in the Removal of Dye from Aqueous Solution, *Colloids and Surfaces B: Biointerfaces*, **101**: 210-214(2013).

[20] Martín M., Salazar P., Villalonga R., Campuzano S., Pingarrón J.M., González-Mora J.L., Preparation of Core–Shell Fe_3O_4@poly(dopamine) Magnetic Nanoparticles for Biosensor Construction, *Journal Of Materials Chemistry B*, **2**: 739-746 (2014).

[21] Sergi A., Shemirani F., Alvand M., Tajbakhshian A., Graphene Oxide Magnetic Nanocomposites for the Preconcentration of Trace Amounts of Malachite Green from Fish and Water Samples Prior to Determination by Fiber Optic-Linear Array Detection Spectrophotometry, *Analytical Methods*, **6**: 7744-7751 (2014).

[22] Zhu B., Edmondson S., Polydopamine-Melanin Initiators for Surface-Initiated ATRP, *Polymer*, **52**: 2141-2149 (2011).

[23] Mittal H., Mishra S.B., Gum Ghatti and Fe₃O₄ Magnetic Nanoparticles Based Nanocomposites for the Effective Adsorption of Rhodamine B, *Carbohydrate Polymers*, **101**: 1255-1264 (2014).

[24] Chang Y.P., Ren C.L., Qu J.C., Chen X.G., Preparation and Characterization of Fe₃O₄/Graphene Nanocomposite and Investigation of Its Adsorption Performance for Aniline and p-Chloroaniline, *Applied Surface Science*, **261**: 504-509 (2012).

[25] Wang Y., Ma X., Ding C., Jia L., pH-Responsive Deoxyribonucleic Acid Capture/Release by Polydopamine Functionalized Magnetic Nanoparticles, *Analytica Chimica Acta*, **862**: 33-40 (2015).

[26] Giles C.H., MacEwan T.H., Nakhwa S.N., Smith D., Studies in Adsorption. Part XI. A System of Classification of Solution Adsorption Isotherms, and Its use in Diagnosis of Adsorption Mechanisms and in Measurement of Specific Surface Areas of Solids, *Journal of the Chemical Society*, **786**: 3973-3993 (1960).

[27] Tsai W.T., Chang Y.M., Lai C.W., Lo C.C., Adsorption of Ethyl Violet Dye in Aqueous Solution by Regenerated Spent Bleaching Earth, *Journal of Colloid and Interface Science*, **289**: 333-338 (2005).

[28] Sprynskyy M., Buszewski B., Terzyk A.P., Namieśnik J., Study of the Selection Mechanism of Heavy Metal (Pb²⁺, Cu²⁺, Ni²⁺, and Cd²⁺) Adsorption on Clinoptilolite, *Journal of Colloid and Interface Science*, **304**: 21-28 (2006).

[29] Lagergren S., About the Theory of so-Called Adsorption of Soluble Substances, *Kungliga Svenska Vetenskapsakademiens Handlingar*, **24**: 1-39 (1989).

[30] Ho Y.S., McKay G., The Kinetics of Sorption of Basic Dyes from Aqueous Solution by Sphagnum Moss Peat, *The Canadian Journal of Chemical Engineering*, **76**: 822-827 (1998).

[31] Vadivelan V., Kumar K.V., Equilibrium, Kinetics, Mechanism, and Process Design for the Sorption of Methylene Blue Onto Rice Husk, *Journal of Colloid and Interface Science*, **286**: 90-100 (2005).

[32] Ho Y.S., Second-Order Kinetic Model for the Sorption of Cadmium Onto Tree Fern: A Comparison of Linear and Non-Linear Methods, *Water Research*, **40**: 119-125 (2006).

[33] Ho Y.S., McKay G., Pseudo-Second Order Model for Sorption Processes, *Process Biochemistry*, **34**: 451-465 (1999).

[34] Ramesha G.K., Vijaya Kumara A., Muralidhara H.B., Sampath S., Graphene and Graphene Oxide as Effective Adsorbents Toward Anionic and Cationic Dyes, *Journal of Colloid and Interface Science*, **361**: 270-277 (2011).

[35] Fan L., Luo C., Li X., Lu F., Qiu H., Sun M., Fabrication of Novel Magnetic Chitosan Grafted with Graphene Oxide to Enhance Adsorption Properties for Methyl Blue, *Journal of Hazardous Materials*, **215–216**: 272-279 (2012).

[36] Langmuir I., The Adsorption of Gases on Plane Surfaces of Glass, Mica and Platinum, *Journal of the American Chemical Society*, **40**: 1361-1403 (1918).

[37] Afkhami A., Moosavi R., Madrakian T., Preconcentration and Spectrophotometric Determination of Low Concentrations of Malachite Green and Leuco-Malachite Green in Water Samples by High Performance Solid Phase Extraction Using Maghemite Nanoparticles, *Talanta*, **82**: 785-789 (2010).

[38] Peng L., Qin P., Lei M., Zeng Q., Song H., Yang J., Shao J., Liao B., Gu J., Modifying Fe₃O₄ Nanoparticles with Humic Acid for Removal of Rhodamine B in Water, *Journal of Hazardous Materials*, **209–210**: 193-198 (2012).

[39] Lata H., Mor S., Garg V.K., Gupta R.K., Removal of a Dye from Simulated Wastewater by Adsorption Using Treated Parthenium Biomass, *Journal of Hazardous Materials*, **153**: 213-220 (2008).

[40] H. Lata, V.K. Garg, R.K. Gupta, Adsorptive Removal of Basic dye by Chemically Activated Parthenium Biomass: Equilibrium and Kinetic Modeling, *Desalination*, **219**: 250-261 (2008).

[41] Khan T.A., Dahiya S., Ali I., Use of Kaolinite as Adsorbent: Equilibrium, Dynamics and Thermodynamic Studies on the Adsorption of Rhodamine B from Aqueous Solution, *Applied Clay Science,* **69**: 58-66 (2012).

[42] Al-Rashed S.M., Al-Gaid A.A., Kinetic and Thermodynamic Studies on the Adsorption Behavior of Rhodamine B Dye on Duolite C-20 Resin, *Journal of Saudi Chemical Society*, **16**: 209-215 (2012).

[43] Hou M.F., Ma C. X., Zhang W.D., Tang X.Y., Fan Y.N., Wan H.F., Removal of Rhodamine B using Iron-Pillared Bentonite, *Journal of Hazardous Materials*, **186**: 1118-1123 (2011).

[44] Liu H., Ren X., Chen L., Synthesis and Characterization of Magnetic Metal–Organic Framework for the Adsorptive Removal of Rhodamine B from Aqueous Solution, *Journal of Industrial and Engineering Chemistry*, **34**: 278-285 (2016).

[45] Naseri A., Barati R., Rasoulzadeh F., Bahram M., Studies on Adsorption of Some Organic Des from Aqueous Solution Onto Graphene Nanosheets, *Iranian Journal of Chemistry and Chemical Engineering (IJCCE), 34*: 51-60 (2015).

[46] Rahimi-Kooh M.R., Khairud-Dahri M., Lim L.B.L., The Removal of Rhodamine B Dye from Aqueous Solution Using Casuarina equisetifolia Needles as Adsorbent, *Cogent Environmental Science*, **2**: 1140553 (2016).

[47] Saini J., Garg V.K., Gupta R.K., Kataria N., Removal of Orange G and Rhodamine B Dyes from Aqueous System Using Hydrothermally Synthesized Zinc Oxide Loaded Activated Carbon (ZnO-AC), *Journal of Environmental Chemical Engineering*, **5**: 884–892 (2017).

[48] El Haddad M., Mamouni R., Saffaj N., Lazar S. Evaluation of Performance of Animal Bone Meal as a New Low Cost Adsorbent for the Removal of a Cationic Dye Rhodamine B from Aqueous Solutions, *Journal of Saudi Chemical Society*, **20**: S53-S59 (2016).

28